DOI 10.1515/hsz-2012-0234 — Biol. Chem. 2012; 393(11): 1341–1355

Reto Walser, Jörg H. Kleinschmidt, Arne Skerra and Oliver Zerbe*

β-Barrel scaffolds for the grafting of extracellular loops from G-protein-coupled receptors

Abstract: Owing to the difficulties in production and purification of G-protein-coupled receptors (GPCRs), relatively little structural information is available about this class of receptors. Here we aim at developing small chimeric proteins, displaying the extracellular ligand-binding motifs of a human GPCR, the Y receptor. This allows the study of ligand-receptor interactions in simplified systems. We present comprehensive information on the use of transmembrane (OmpA) and soluble (Blc) β-barrel scaffolds. Whereas Blc appeared to be not fully compatible with our approach, owing to problems with refolding of the hybrid constructs, loop-grafted versions of OmpA delivered encouraging results. Previously, we described a chimeric construct based on OmpA displaying all three extracellular Y1 receptor loops in different topologies and showing moderate affinity to one of the natural ligands. Now, we present detailed data on the interaction of these constructs with several Y receptor ligands along with data on new constructs. Our findings suggest a common binding mode for all ligands, which is mediated through the C-terminal residues of the peptide ligand, supporting the functional validity of these hybrid receptors. The observed binding affinities, however, are well below those observed for the natural receptors, clearly indicating limitations in mimicking the natural systems.

Keywords: membrane proteins; mini-receptor; neurohormones; structural biology; Y receptors.

***Corresponding author: Oliver Zerbe,** Institute of Organic Chemistry, University of Zurich, Winterthurerstrasse 190, CH-8057 Zurich, Switzerland, e-mail: oliver.zerbe@oci.uzh.ch
Reto Walser: Institute of Organic Chemistry, University of Zurich, Winterthurerstrasse 190, CH-8057 Zurich, Switzerland
Jörg H. Kleinschmidt: Department of Biophysics, Institute of Biology, Heinrich-Plett-Str. 40, D-34132 Kassel, Germany
Arne Skerra: Munich Center for Integrated Protein Science, CIPS-M, and Lehrstuhl für Biologische Chemie, Technische Universität München, D-85350 Freising-Weihenstephan, Germany

Introduction

G-protein-coupled receptors (GPCRs) represent one of the most important classes of cell-surface receptors and constitute prevalent targets for pharmaceutical drugs (Tyndall and Sandilya, 2005; Congreve and Marshall, 2010). The crystal structures of several GPCRs (Katritch et al., 2012) have deepened our understanding of this biologically important class of proteins.

The structure of GPCRs can be described as an extracellular N-terminal domain, attached to a heptahelical segment embedded in the plasma membrane, which is followed by a cytosolic domain. The seven transmembrane (TM) helices are on either side connected by three intra- (i1 to i3) or extracellular (e1 to e3) loops, respectively. Although the overall topology of the heptahelical bundle is generally conserved in GPCRs with known structure, the extracellular loops are largely unstructured (for a comparison, see reviews by Hanson and Stevens, 2009 and Peeters et al., 2011). Furthermore, increased crystallographic B-factors in the extracellular loops are often observed. Conformational flexibility has been interpreted to play a role for ligand binding (Koshland, 1958).

Ligands of those GPCRs whose X-ray structures have been determined recently are usually small molecules that bind to a pocket among the helix bundle within the transmembrane region. Only one high-resolution structure of a GPCR bound to a small peptidic antagonist is available so far (Wu et al., 2010). In general, peptide ligand-binding sites are believed to be part of the extracellular loops and the extracellular N-terminal domains (Lagerstrom and Schioth, 2008).

Despite recent progress in X-ray structure elucidation, the expression, purification and refolding generally still present major hurdles in the structural study of GPCRs. Successful NMR studies of GPCRs are yet missing. This is only in part due to the inherent problems of NMR for the investigation of large molecules, such as line broadening and signal overlap. In addition, slow conformational dynamics often severely deteriorate the quality of the spectra.

In light of the fundamental problems for studying entire GPCRs by solution NMR, we aim at establishing a model system in which the extracellular loops of a peptide-binding GPCR are grafted onto a robust protein scaffold that is better amenable to NMR spectroscopy than the heptahelical TM bundle. Such a scaffold should (i) display all loops in a favorable topology, (ii) be expressible in high yields in a microbial host, and (iii) be easy

to purify, solubilize and/or refold. Such a chimeric receptor may be useful for pharmacological studies with regard to the strength and specificity of ligand binding or to the competitive binding behavior between various agonists and antagonists.

Recently, we described the development of a model that mimics the extracellular domains of the human Y receptors based on a β-barrel scaffold from the *Escherichia coli* outer membrane protein A (OmpA) (Walser et al., 2011). The model takes advantage of the membrane-integral β-barrel fold of OmpA and displays grafted loops in a favorable topology. The Y receptors are targeted by neurohormones from the neuropeptide Y family: neuropeptide Y (NPY), peptide YY (PYY) and pancreatic polypeptide (PP) (Larhammar, 1996a). To date, four different subtypes of receptors have been characterized (Y1, Y2, Y4 and Y5; Larhammar, 1996b; Larhammar and Salaneck, 2004), which are associated with different pharmacological effects. In these, the three extracellular loops, and possibly also the N-terminal domain, are proposed to be involved in ligand binding (Zou et al., 2008).

We now describe the development of this receptor model in much more detail. As scaffolds we have initially employed two different, yet structurally related β-barrel proteins, the soluble bacterial lipocalin (Blc) (Bishop, 2000; Schiefner et al., 2010) and OmpA (Tamm et al., 2003) from *E. coli*. We demonstrate that all three extracellular Y1 receptor loops and its N-terminus can be successfully transferred to the OmpA scaffold.

Results

Design aspects

To date, structural details at atomic resolution are available for nine major different GPCRs (for a summary see the supplementary material online). We selected the N-termini and extracellular loops of the Y receptors based on the predicted topology as annotated in the GPCRDB (e.g., http://www.gpcr.org/7tm/proteins/npy1r_human for the human Y1 receptor). In the case of the human Y1 receptor, the extracellular loops comprise 13 and 14 residues for e1 (Y99 to M111) and e3 (F284 to N297), respectively, and 34 residues for e2 (Q176 to S209). The predicted N-terminal domains of the Y1, Y2 and Y4 receptors are the first 40, 50 and 41 residues, respectively.

The rationale for the design of the loop-grafted receptor models was as follows. First, we defined anchor points as the positions of the terminal Cα atoms of the α-helix or the β-strand that is connected to a loop. The mutual distances between these anchor points define the overall topology of the set of extracellular loops. Figure 1 depicts a comparison of the distances between the anchor points on the extracellular side for a set of 10 different GPCR crystal structures with known structure at the onset of our study (for a list see the materials and methods section). The spacing between the anchor points for the three extracellular loops is on average 13 Å for e1 and e2 and 14 Å for e3, with a narrow distribution of ±3 Å. The distances between anchor points that are not part of the same loop are much less conserved, indicating that the relative positions of two helices anchoring the same extracellular loop is more conserved than the relative positions between helices not directly connected.

A similar analysis was conducted for the available high-resolution structures of Blc (Campanacci et al., 2004; Schiefner et al., 2010) and OmpA (Pautsch and Schulz, 1998, 2000). Because both published OmpA X-ray structures lack defined electron density for a substantial number of residues located in the extracellular loops, we mostly relied on the NMR structures for this protein (Arora et al., 2001; Cierpicki et al., 2006). Figure 1 depicts a statistical analysis of the distances observed in the crystal structure of Blc (Campanacci et al., 2004) and the 10 lowest energy conformers of two NMR structures of OmpA (Arora et al., 2001; Cierpicki et al., 2006), as well as a shortened loop construct of the OmpA scaffold (Johansson et al., 2007).

A comparison of the pairwise distances between anchor points in GPCRs and these scaffold proteins revealed that the distance distribution observed in the GPCRs falls within the distribution observed for the OmpA structures and is also close to the distances observed for Blc, suggesting that the β-barrels of Blc and OmpA might indeed provide suitable frameworks for grafting the extracellular loops of GPCRs. Whereas the distances between directly connected anchor points are between 10 and 17 Å in OmpA, in Blc those distances are significantly shorter: approximately 5 Å for three anchor point pairs and 10 Å for the fourth pair. GPCRs possess three, whereas OmpA carries four extracellular loops, leaving at least one 'acceptor' site in the scaffold unoccupied. To rule out interference with the remaining native loop, it was replaced by a minimal turn-inducing motif of one to two residues compatible with the OmpA β-barrel structure (Koebnik, 1999a).

Blc construct design

We have previously demonstrated that the extracellular N-terminal domain of the Y4 receptor (NY4) interacts with

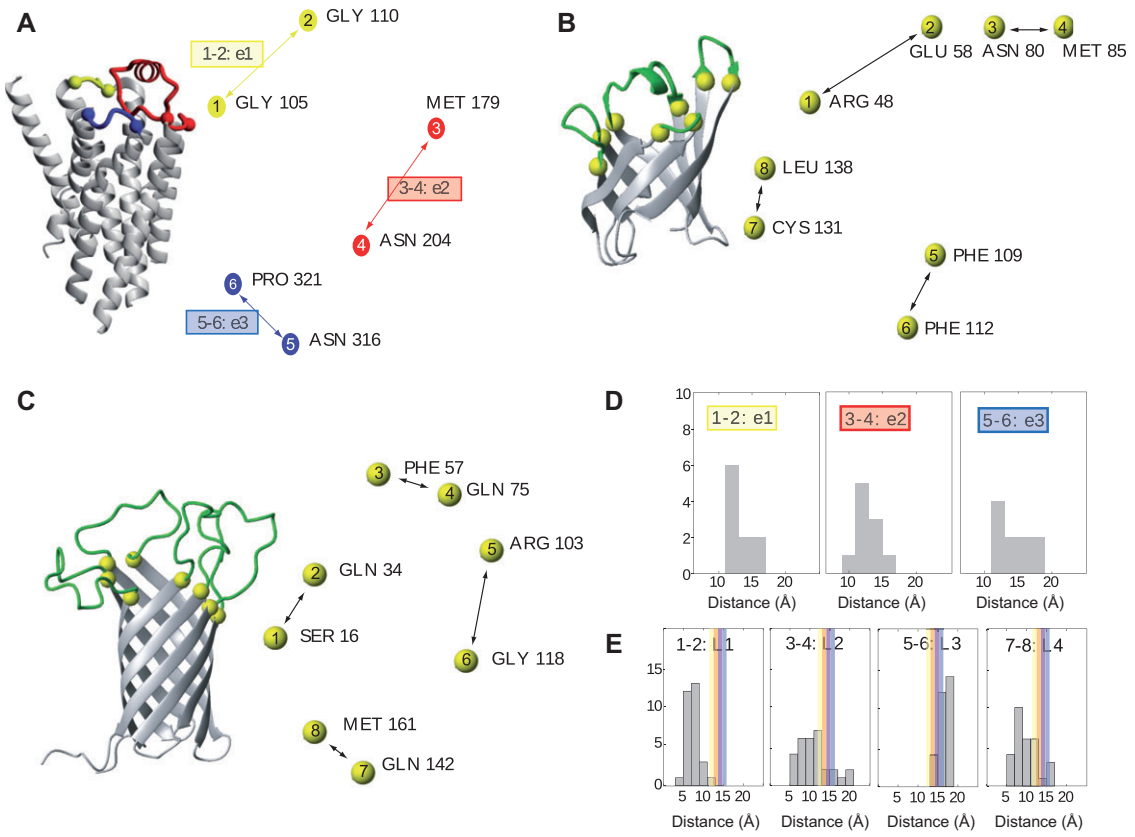

Figure 1 Geometries of GPCRs and β-barrel proteins.
(A) Ribbon representation of bovine rhodopsin with the first, second and third extracellular loops (e1–3) colored yellow, red and blue, respectively. On the right the arrangement of the extracellular loop anchor points is presented as viewed from the extracellular side (same color coding used as in the ribbon representation). Each anchor point is labeled by its terminal/initial residue and the TM-helix to which it belongs. (B) Ribbon representation of Blc with its four variable loops colored green and the anchor points yellow. On the right the arrangement of the loop anchor points is presented as viewed from the top (same color coding as in ribbon representation). Directly connected anchor points are indicated by black arrows. For clarity the N-terminal 3_{10}-helix and the C-terminal α-helix of Blc is omitted in the ribbon representation. (C) Same representation as in (B) for OmpA. (D) Histograms of the distances between the anchor points for extracellular loops 1, 2 and 3 as found in a set of 10 GPCR crystal structures (see the supplementary material and methods online for a full list) (top panel) and (E) for the extracellular loops in the NMR structures of two OmpA structures and one loop-shortened OmpA construct (10 conformers each) (bottom panel). Average distances between the anchor points for the e1-, e2- and e3-loop in the GPCR structures are indicated by yellow, red and blue bars, respectively.

PP (Zou et al., 2008, 2009). Because of its well-behaved nature in terms of expression and stability, we have initially chosen the Y2 receptor N-terminus (NY2) for our studies aiming at determining suitable attachment points to the Blc scaffold. Accordingly, we fused the NY2 domain to different positions in the N-terminal region of Blc. In these constructs, varying portions of the Blc N-terminus were replaced with NY2 to test how close a grafted N-terminal sequence can be brought to the first strand of the Blc β-barrel, without impairing its fold. The tolerance of the scaffold towards the fused sequence was determined by [^{15}N,^{1}H]-HSQCs (see Figure 2). Moving the fusion point between NY2 and Blc too close to the characteristic 3_{10}-helix (<10 residues) that in many lipocalins precedes the β-barrel (Flower et al., 2000) resulted in insoluble constructs, whereas fusion at more N-terminal positions was well tolerated. However, no interaction of the chimera with NPY family neurohormones could be detected. We also attempted to investigate whether the interaction detected between NY4 and PP (Zou et al., 2008) could be reproduced in the context of the Blc scaffold, but no stably folded fusion protein with NY4 could be obtained (data not shown). We also set out to incorporate the extracellular loops of the Y1 receptor (e1Y1 to e3Y1), but the Blc scaffold did not tolerate the necessary modifications in its loops.

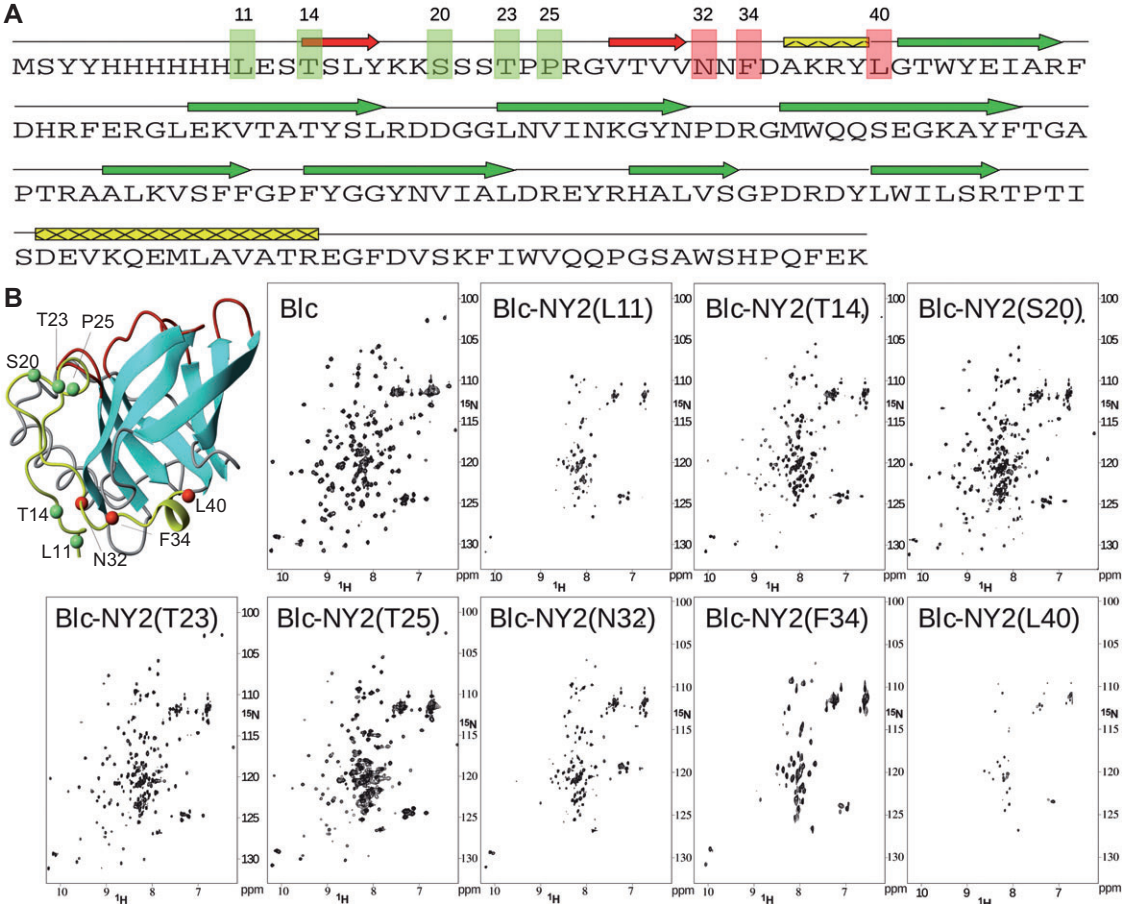

Figure 2 Summary of Y2 receptor N-terminus grafting attempts using Blc.
(A) Blc sequence with colored arrows indicating the β-strand secondary structural elements in the crystal structure. Red: additional two-stranded β-sheet which has arisen as a cloning artifact (Schiefner et al., 2010); yellow: N-terminal 3_{10}- and C-terminal α-helix, both characteristic for the lipocalin fold; green: eight-stranded β-barrel, the central motif of the lipocalin fold. The sequence 23–177 corresponds to the natural Blc protein, to which a His_6 tag was appended at the N-terminus and a *Strep*-tag II at the C-terminus. Residues to which the NY2 sequence has been N-terminally fused are shaded in green or red, indicating constructs resulting in soluble or insoluble protein, respectively. (B) Ribbon representation of Blc with the residues to which the NY2 sequence was N-terminally fused colored in green or red, as in panel (A). The [^{15}N,^{1}H]-HSQC spectra of Blc and the respective NY2-grafted/fused constructs are depicted next to the structure. Properly folded constructs are characterized by good signal dispersion in the spectra.

OmpA construct design

Our initial studies concentrated on probing the compatibility of the Y receptor extracellular loops with the OmpA scaffold. Considering that most of the data from mutagenesis studies are available for the Y1 receptor, we exchanged each of the four extracellular loops of OmpA with each of the three eY1 loops individually to generate 12 constructs altogether, dubbed 'one-loop exchange constructs'. Further, we constructed a series of OmpA mutants in which a single eY1 loop was grafted into one OmpA acceptor site while the other three sites were filled with a minimal turn-inducing motif (Koebnik, 1999b). These were called 'one-loop graft constructs'. All constructs could be expressed in *E. coli*, solubilized in urea and refolded (see Figure S1 in the supplementary material online), indicating that OmpA is suitable as a generic scaffold for grafting individual eY1 loops, both in the presence and absence of the other three of its natural loops.

In principle, the set of three eY1 loops can be arranged in 24 different ways (4×3×2) on the OmpA scaffold according to this approach. To avoid unsuitable constructs when combining the individually grafted loops, we calculated a 'mismatch score' accounting for the distance mismatches of all relevant anchor points between the model scaffold and the GPCRs (see Figure 3). Among the candidates with low mismatch scores, only those with a correct topological

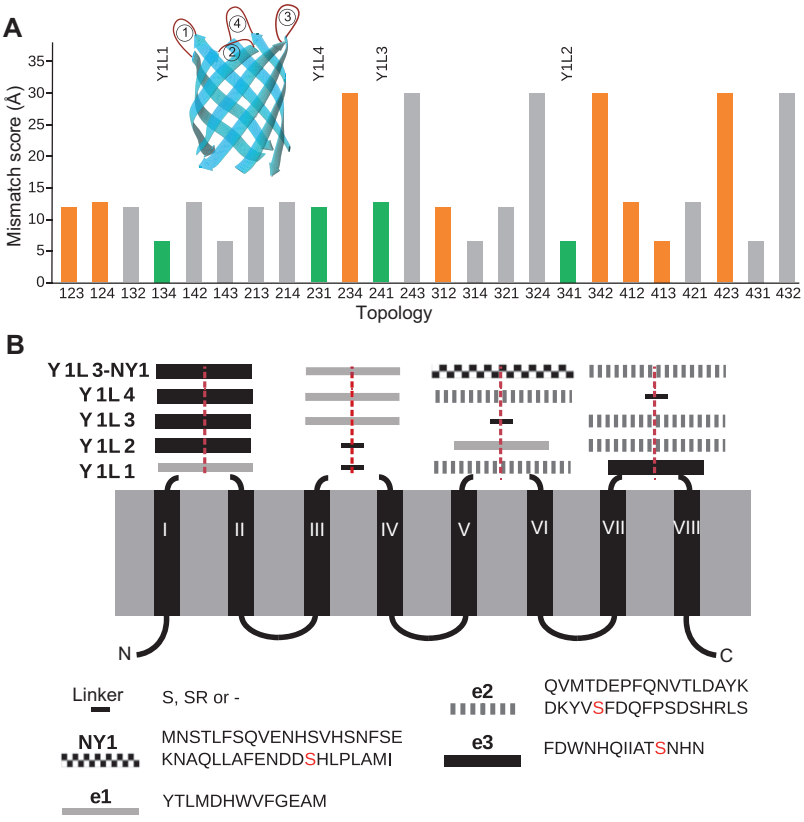

Figure 3 Design of receptor constructs.
(A) Calculation of the mismatch score (in Å) for all 24 possible 'receptor constructs' (for a description of the calculation procedure see materials and methods section). Constructs displaying the Y receptor extracellular loops in an appropriate topological orientation for grafting are colored. The four chimeric GPCR-OmpA constructs selected for expression (Y1L1, Y1L2, Y1L3 and Y1L4) are marked in green. (B) Topography for the selected constructs of the three e1–3 loops of Y1 on the eight-stranded OmpA β-barrel. The remaining unused fourth loop of the OmpA scaffold was replaced by a short linker sequence. Amino acid sequences for the three Y1 loops as well as the short linker are depicted at the bottom. Serine residues highlighted in red correspond to cysteine side chains in the natural Y1 sequences, which were substituted to avoid formation of undesired disulfide crosslinks.

loop arrangement (i.e., the C-terminus of e1 to be followed by the N-terminus of e2 in a clockwise manner and so on) were considered. Four of those arrangements were selected and will be referred to in the following as 'receptor constructs', abbreviated as Y1L1, Y1L2, Y1L3 and Y1L4 (see Figure 3).

The initial topological analysis of the anchor point distances revealed that although the pairwise distances for each loop in the known GPCR structures fall within the range of those observed in OmpA, the overall match is not perfect. To account for these structural differences, additional flexible linker residues at the termini of the loops were introduced by inserting glycine-serine spacers of different lengths. Based on the Y1L3 topology six constructs were designed: two in which each Y1 receptor loop was flanked on both sides by a Ser-Gly dipeptide or a Ser-Gly-Ser-Gly tetrapeptide (Y1L3-GS and Y1L3-GSGS), respectively, two where only the short e1- and e3-loops were flanked by these spacers (Y1L3-gs and Y1L3-gsgs), and two where only the longer e2-loop was equipped with the spacers (Y1L3-e2gs and Y1L3-e2gsgs).

Notably, all these constructs lack the N-terminal receptor domain, which may also be involved in ligand binding (Robin-Jagerschmidt et al., 1998; Wieland et al., 1998; Zou et al., 2008). Unfortunately, in OmpA the N-terminus of the β-barrel is located opposite to the (extracellular) face used for grafting. We inserted the sequence of the N-terminal Y1 receptor domain (NY1) into the third, so far 'empty' acceptor position of Y1L3, flanked by an N-terminal $(Gly\text{-}Ser)_3$ and a 3C protease cleavage site, allowing the *in situ* generation of a free N-terminus via proteolytic cleavage after refolding (construct Y1L3-NY1 in Figure 3).

Biosynthetic aspects of hybrid GPCR-OmpA constructs

All these constructs were purified, solubilized and refolded in unlabeled and ^{15}N-labeled form from inclusion bodies produced in *E. coli* with yields of ~200 and ~100 mg/l of LB rich medium or ^{15}N-labeled M9 minimal medium, respectively. The folding state of OmpA was monitored by SDS-PAGE in which the sample was mixed with SDS sample buffer but not heated prior to loading on the gel, leaving the OmpA fold intact and referred to here as 'non-denaturing SDS-PAGE' (Reithmeier and Bragg, 1974; Schweizer et al., 1978). During refolding screens, solutions of the urea-denatured chimeric OmpA were diluted into different buffers containing various detergents at concentrations above their critical micellar concentrations (cmc) and at detergent/protein ratios >500 (for a list of the relevant biophysical parameters, see Table S1 in the supplementary material online).

All of the 12 'one-loop exchange constructs' and 6 of the 'one-loop graft constructs', as well as the 4 selected 'receptor constructs' were expressed, purified and their refolding capability was assessed by non-denaturing SDS-PAGE (see Figure 4). Whereas the expression level of all 22 constructs was similar to that of wild type (wt)-OmpA, the refolding efficiency was clearly lower for some of these constructs. Nevertheless, each of the 22 constructs could be refolded at least to 50% (data not shown). Generally, refolding efficiency increased with increasing pH (Kleinschmidt et al., 1999). Whereas for some constructs rapid dilution of the urea-denatured protein solution into detergent buffer at high pH 10.0 resulted in nearly complete refolding, some constructs required more gentle conditions of slow dilution at a lower temperature of 4°C.

In the Y1L3-NY1 construct complete refolding under similar conditions of pH and detergent was possible (see Figure 5B). After refolding in DHPC micelles, Y1L3-NY1 was incubated with 3C protease and the efficiency of cleavage and integrity of the β-barrel were assessed by denaturing and non-denaturing SDS-PAGE, respectively. As can be seen in Figure 5B, bands corresponded closely to the expected sizes. Y1L3-NY1 refolded in DHPC micelles showed the same electrophoretic mobility before and after treatment with 3C protease, indicating integrity of its tertiary fold even after cleavage. The appearance of two bands around 14 kDa and the concomitant complete disappearance of the band at 27 kDa under denaturing SDS-PAGE conditions proved that the proteolytic cleavage was highly efficient (for results with alternative detergents see Figure S2 in the supplementary material online).

Whenever folded forms of the chimeric OmpA constructs were detected by SDS-PAGE, the presence of tertiary structure and formation of the β-barrel was also apparent from the large signal dispersion in the [^{15}N,^{1}H]-HSQC spectra of these preparations (for [^{15}N,^{1}H]-HSQC spectra of the four receptor constructs Y1L1-4, see Figure S3 in the supplementary material online).

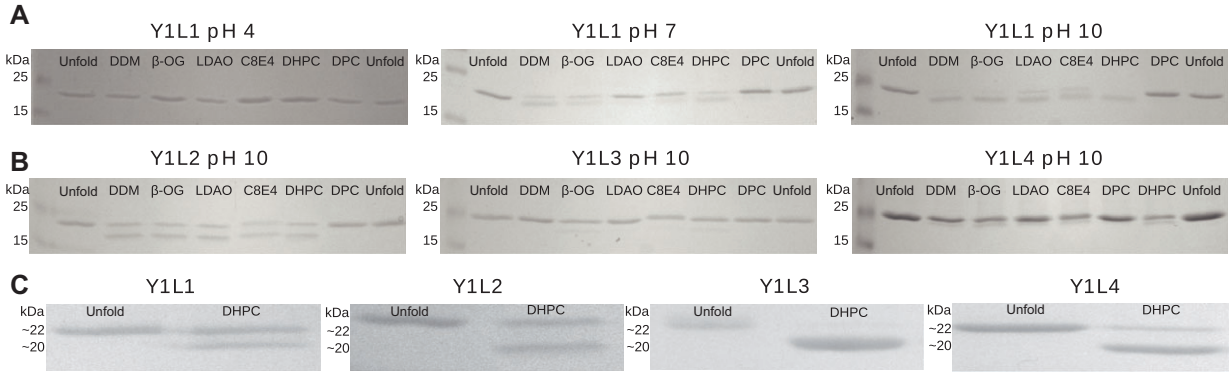

Figure 4 Folding properties of grafted receptor constructs using non-denaturing SDS-PAGE.
(A) pH dependence of the refolding efficiency of Y1L1 in a variety of different detergents (DDM: α-dodecyldimaltoside, β-OG: β-octylglucoside, C8E4: tetraethyleneglycol monooctylether, LDAO: N-lauryldimethyl amineoxide, DPC: dodecylphosphocholine, DHPC: dihexanoylphosphatidylcholine). Although refolding is not efficient in all detergents, a clear trend to increased efficiency apparent from the presence of a lower band different from the heat-denatured (unfolded) species at higher pH is observed. (B) Whereas Y1L1 and Y1L2 can be refolded with fairly high efficiency at pH 10 in most detergents tested, corresponding efficiencies for Y1L3 and Y1L4 are much lower. (C) Optimization of the refolding procedure towards more gentle conditions (lower temperature, slow dilution of the denatured stock solution) results in increased refolding efficiency especially for Y1L3 and Y1L4.

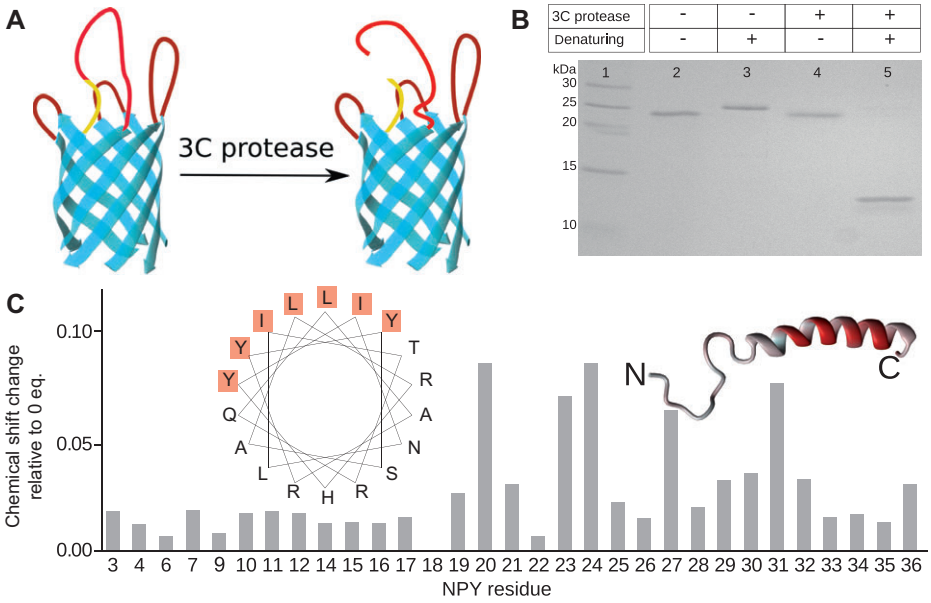

Figure 5 Interaction studies with the 'split' receptor model that additionally displays the N-terminal domain of Y1, Y1L3-NY1. (A) Schematic representation of the construct. The OmpA β-barrel is shown in cyan, the grafted eY1 loops in dark red, the $(Gly\text{-}Ser)_3$-linker and 3C protease cleavage site in yellow and NY1 in red. (B) SDS-PAGE of Y1L3-NY1 under different conditions: a different migration behavior under non-denaturing (lane 2) and denaturing (lane 3) conditions indicates successful refolding of the construct. After treatment with 3C protease the construct shows the same migration behavior (lane 4) as before (lane 2) under non-denaturing conditions. Under denaturing conditions two bands with sizes of approximately 14 kDa can be seen after cleavage with 3C protease (lane 5). (C) The chemical shift changes observed in the [^{15}N,^{1}H]-HSQC spectrum of NPY upon addition of 20 Eq. of cleaved Y1L3-NY1 protein plotted for each residue and color-coded onto the α-helical structure of NPY where gray indicates no change and the intensity of red is proportional to the chemical shift change. Changes are most prominent on one side of the helix. A helical wheel representation of the C-terminal α-helix (L17-Q34) of NPY shows that this side exclusively comprises hydrophobic and aromatic residues.

Interaction studies of neurohormones of the NPY family with chimeric Y1-OmpA receptor constructs

Binding of NPY, PYY and PP to the receptor constructs was tested using chemical shift mapping or saturation transfer difference (STD) (Mayer and Meyer, 1999, 2001) techniques. ^{15}N-labeled neurohormones (for assignments, see Table S2 in the supplementary material online) were titrated with unlabeled receptor constructs. The resulting changes for the NPY spectra upon addition of 20 Eq. of the chimeric receptor constructs are depicted in Figure 6. No interactions could be detected with Y1L1 or Y1L2, whereas Y1L3 and Y1L4 induced significant changes in the [^{15}N,^{1}H]-HSQC spectra of NPY when present in excess. Interestingly, no shift in peak positions, but a decrease in peak intensities was observed. This finding is consistent only with an exchange process slow on the NMR time scale, which usually results in two sets of peaks, one corresponding to the bound and the other to the non-bound form. We suspect that excessive broadening of the resonances due to small conformational fluctuations in the receptor-bound state or a large number of different states that do not interconvert fast on the NMR time scale has led to the disappearance of the bound-state signals.

Figure 6 depicts the volume changes of the peaks from the neurohormones upon titration with an excess of Y1L3 (for similar results obtained with the SG linker versions, see Figure S4 in the supplementary material online). The data clearly indicate that the C-terminal residues of the peptide were much more affected by interaction with the chimeric receptor than those of the N-terminus. In agreement with previous studies (Beck-Sickinger et al., 1994), this indicated that the C-terminal α-helix of the neurohormone is involved in receptor binding. Despite the qualitative similarities of the peak volume changes between all three neurohormones tested, the attenuations were less pronounced for PYY and, in particular, for PP than for NPY. Considering that the binding profile of PP to the Y receptor subtypes has been shown to be different from the binding profiles of NPY and PYY (Larhammar and Salaneck, 2004), this may indicate differences in the binding mode in our model system, too.

Specificity of the interaction was corroborated by a competition experiment with unlabeled NPY (Figure 6C)

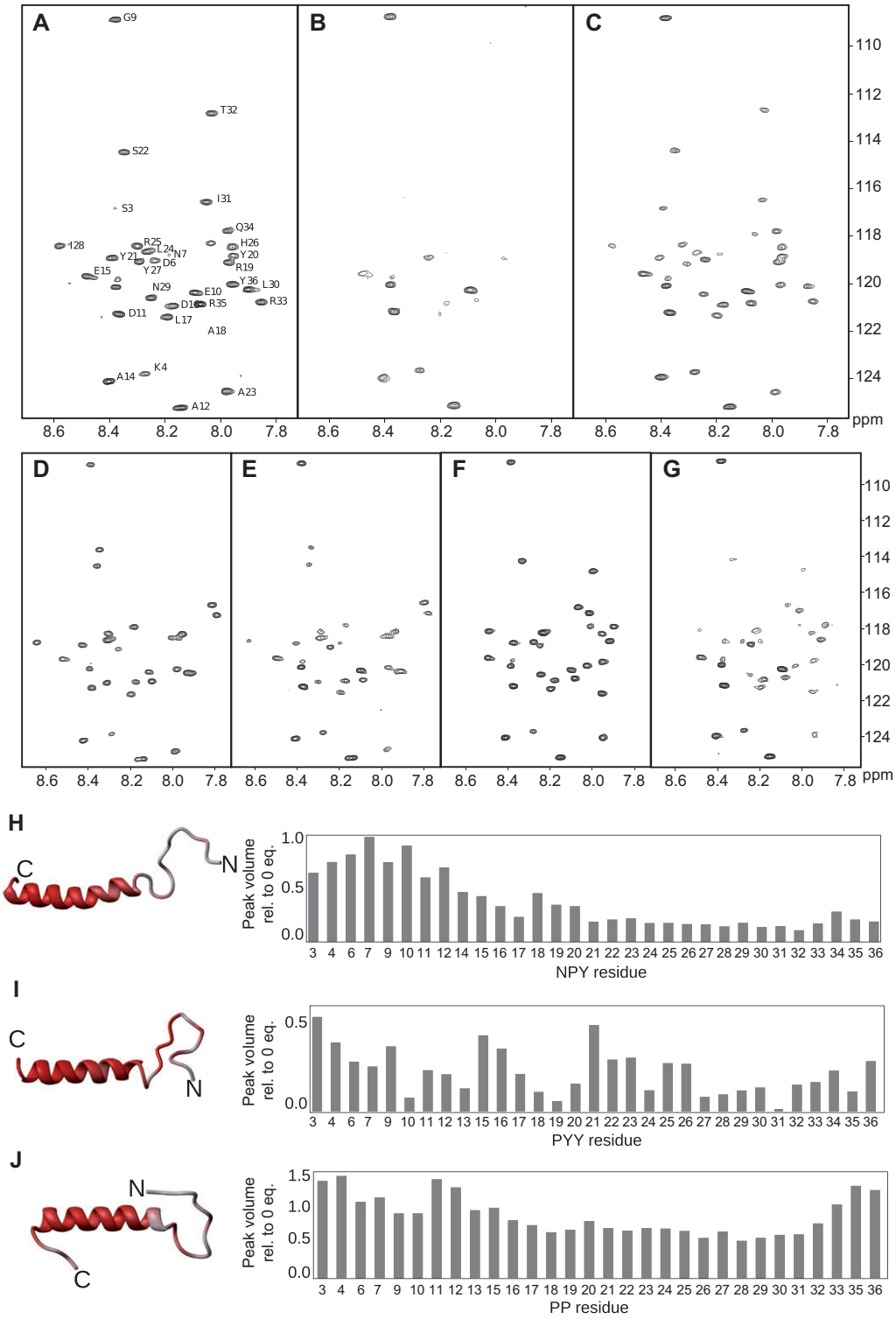

Figure 6 Interaction studies between peptide hormones and receptor constructs using NMR.
[^{15}N,^{1}H]-HSQC spectra of the ^{15}N-NPY in 3% DHPC, 20 mM phosphate pH 6.5, 100 mM NaCl at 310 K (A) in the absence, (B) in the presence of 20 Eq. of unlabeled Y1L3 protein and (C) in presence of 20 Eq. of unlabeled Y1L3 protein and 50 Eq. of unlabeled NPY. [^{15}N,^{1}H]-HSQC spectra of mutant peptide ^{15}N-NPY-R35L (D) in the absence, (E) in the presence of 20 Eq. of unlabeled Y1L3 protein. [^{15}N,^{1}H]-HSQC spectra of mutant peptide ^{15}N-NPY-R33L (F) in the absence, (G) in the presence of 20 Eq. of unlabeled Y1L3. The relative residue-specific volume change of (H) NPY, (I) PYY and (J) PP resonances upon addition of Y1L3 protein plotted for each residue. The relative volume change is color-coded onto the structure of the (micelle-bound) species of each neurohormone, with gray stretches indicating no change and the intensity of the red color being proportional to the relative volume change.

(Walser et al., 2011). Furthermore, binding assays with NPY-R33L and NPY-R35L, two mutants of NPY that exhibit much reduced affinity to the Y1 receptor *in vivo* (Beck-Sickinger et al., 1994), were conducted. These mutant NPY peptides displayed a markedly decreased affinity for Y1L3 as visible from the reduced attenuation of peaks for the C-terminal residues (see Figure 6D–G). In summary, these findings confirmed a specific interaction of the neurohormones of the NPY family with the chimeric GPCR-OmpA receptor construct Y1L3.

Interestingly, the chemical shift mapping data from titration of ^{15}N-NPY with cleaved or uncleaved Y1L3-NY1 showed a behavior very different from Y1L3, revealing shifts in the positions of certain peaks (see Figure 5C and Figure S5 in the supplementary material online). Large chemical shift changes were exclusively observed in the C-terminal helix of NPY, showing a pronounced i+3 or i+4 periodicity, thus indicating an interaction involving residues located on the same side of the helix.

STD experiments conducted with NPY in the presence of Y1L3 or cleaved Y1L3-NY1 showed the most pronounced saturation transfer effects for the aromatic resonances of peptide residues, which – with the exception of the N-terminal Tyr – are all located in the C-terminal half of NPY (Walser et al., 2011).

To obtain further information on the ligand-receptor interactions, all four ^{15}N-labeled receptor constructs Y1L1-4 were mixed with unlabeled NPY (see Figure S6 in the supplementary material online). Surprisingly, the [^{15}N,^{1}H]-HSQC spectra of the all chimeric receptor constructs did not display major changes upon addition of the neurohormone. We speculate that most peaks from the short e1- and e3-loops, which have been proposed to mediate interaction with the peptide hormones (Walker et al., 1994; Merten et al., 2007), are exchange-broadened beyond detection. This view is supported by the observation that the actual number of observed sharp peaks in the receptor constructs, which most likely originate from the flexible loops, is only ~40 out of an expected 60. To verify that resonances from the e1 and e3 loops are absent in the spectra of the receptor-peptide complexes, we attempted to assign the backbone of Y1L3 using perdeuterated protein (see Figure S7 in the supplementary material online).

Characterization of the chimeric receptor species responsible for binding

Because the refolding efficiency of the two apparently functional receptor constructs Y1L3 and Y1L4 was <100%, it is *a priori* not clear whether it was the folded or the unfolded component of the mixture that showed interaction with the neurohormones in the NMR titration experiments. Given the lack of a method to fully separate the folded from the unfolded protein species, we chose to produce Y1L3 under conditions that resulted in the completely unfolded chimeric receptor and repeated the chemical shift mapping experiments on NPY. To this end, 'refolding' was performed at the favorable pH 10, however, in the presence of the detergent DPC which is incapable of inducing refolding. Addition of 30 Eq. of this unfolded Y1L3 preparation in DPC to the NPY neurohormone had a much smaller effect than the addition of 20 Eq. of the (partially) folded Y1L3 in the previous experiments using DHPC as detergent (see Figure S8 in the supplementary material online).

Discussion

Peptide hormone binding to GPCRs is largely mediated through association of the ligand with the extracellular receptor loops (Bockaert and Pin, 1999). Considerable biochemical information on the interactions of the Y receptors with their ligands exists. For example, a complete alanine scan for NPY revealed a drop in affinity towards the human Y1 receptor by approximately four orders of magnitude for point mutations at either Arg33 or Arg35 (Beck-Sickinger et al., 1994). On the receptor side, acidic residues have been proposed to be involved in ionic interactions with these Arg residues of the peptide ligand, most prominently the highly conserved Asp6.59 at the interface of TM6 and e3 (Merten et al., 2007). In addition, it was recently proposed that transient contacts are formed by the peptide with the N-terminal receptor domain, facilitating transfer of the ligand from a membrane-associated state to the binding site of the receptor (Bader and Zerbe, 2005; Zou et al., 2008).

To circumvent the biochemical and spectroscopic problems when studying entire GPCRs, we tested whether the extracellular domains can be transferred onto a suitable more robust protein scaffold. Individual GPCR loop sequences have been investigated previously as free peptides or attached to some support. For example, Yeagle and coworkers structurally characterized peptides corresponding to the extracellular loops of rhodopsin (Yeagle et al., 1997a,b). Similarly, Mierke et al. synthesized peptides comprising the cytosolic loops of the PTH receptor (Mierke et al., 1996). Pham et al. described peptides that contained the sequence of the e1 loop of the sphingosine-1-phosphate

receptor 4 ($S1P_4$) flanked by soluble self-assembling segments that mimicked the helical N-terminus of TM 2 and the C-terminus of TM 3 (Pham et al., 2007). A conceptual disadvantage of these approaches is that the loop-constraining entities are themselves rather flexible. Hence, it was the purpose of the present study to provide a more rigid, three-dimensional scaffold that enforces orientation of the entire set of GPCR loops into a defined overall geometry.

For the success of such an approach the proper choice of the protein scaffold is crucial (Skerra, 2000a). Examples of widely employed protein scaffolds include antibodies (i.e., the immunoglobulin fold represented by single Ig and Ig-like domains; Hudson and Souriau, 2003), protease inhibitors such as Kunitz-type domains (Dennis and Lazarus, 1994), lipocalins (Skerra, 2000b), natural (Brunet et al., 1993) and artificial helix bundles (Houston et al., 1996), as well as smaller peptides rich in disulfide bonds, so-called knottins (Smith et al., 1998). Eight-stranded β-barrel proteins, both soluble and membrane-embedded, display four extracellular loops and usually provide high-folding stability (Skerra, 2000a; Schulz, 2002). Previous work has demonstrated that binding specificity for small and large molecules can be engineered into lipocalins by directed evolution (Skerra, 2000a; Kim et al., 2009; Schonfeld et al., 2009). However, our initial attempts to employ the bacterial lipocalin, Blc (Campanacci et al., 2004; Schiefner et al., 2010), as a scaffold for grafting the extracellular loops of the Y receptor, unfortunately resulted in mutants that could not be efficiently refolded. A likely explanation is that Blc itself has a particularly low thermal stability around 45°C. An interesting alternative candidate in this regard might be the newly discovered thermostable 'slim lipocalin' from a Gram-positive bacterium (Wu et al., 2012). The absence of detergents and the concomitant decrease in molecular weight and lower complexity of the system offers attractive advantages for development of a soluble protein scaffold.

Considering that binding of the neurohormones of the NPY family to the Y receptors has been postulated to occur from a membrane-bound state (Bader and Zerbe, 2005), a membrane-embedded β-barrel scaffold seems to be more suitable despite the above-mentioned technical problems with such systems. OmpA is structurally (Pautsch and Schulz, 2000; Arora et al., 2001) and biochemically (Ried et al., 1994; Kleinschmidt et al., 2011) well characterized, can be easily solubilized with detergents and is of a size still amenable to routine NMR studies.

It is likely that no single heterologous scaffold will perfectly match all the loop geometries encountered in GPCRs. Nevertheless, a statistical comparison of distances between loop anchor points in the solution structures of OmpA and in the available X-ray structures of GPCRs revealed that these distances fall into similar ranges. Taking into account the presumed plasticity of anchoring points in OmpA and the known flexibility of loop residues in the GPCRs, we believe that the β-barrel of OmpA should provide a viable scaffold to present the extracellular loops of many GPCRs. Remaining mismatches of distances in the model may be partially compensated by structural adaptation or by choosing appropriate linkers.

The protein engineering studies described herein demonstrate that OmpA represents a biosynthetically suitable scaffold as most of its mutants could be successfully refolded. For all constructs studied the refolding efficiency generally increased at elevated pH, as previously observed for wt-OmpA (Surrey and Jähnig, 1992; Kleinschmidt et al., 1999). However, the chimeric receptors could not be refolded quantitatively. For all the four designed receptor constructs Y1L1–4, [^{15}N,^{1}H]-HSQC data indicate that the β-barrel has remained intact. This observation corroborates the notion by others (Johansson et al., 2007) and from our previous work (Walser et al., 2011) that OmpA can serve as a generic scaffold for loop-grafting purposes.

NMR chemical shift mapping techniques revealed that some of our chimeric receptor constructs indeed bind the cognate peptides with reasonable affinity. The fact that ^{15}N-labeled NPY can be displaced from the chimeric OmpA receptor constructs with unlabeled NPY in a competition assay strongly argues in favor of a specific interaction with the ligand and against a general mode of lipid association or other non-specific binding events (Walser et al., 2011). This fact is further corroborated by the observation that peptides with reduced affinities for the wild type Y receptors also bound with lower affinity to our recombinant receptor model. Also, the addition of wt-OmpA or of a minimal length OmpA with all four extracellular loops replaced by short, turn-inducing motifs (Koebnik, 1999a) failed to reveal an interaction. Finally, only some of the receptor constructs (Y1L3/Y1L4) bound the peptide ligands whereas others (Y1L1/Y1L2) did not, indicating that the precise arrangements of the loops is indeed important.

Owing to the fact that the neurohormones bind to the micelles with micromolar dissociation constants (Lerch et al., 2005), a precise determination of the K_d for binding the receptor construct is difficult to obtain. The observation of slow exchange on the NMR time scale in the chemical shift mapping experiments however allows to estimate that the affinities of the peptide ligands to the model receptor are lower by approximately three

orders of magnitude when compared to the wild type GPCRs (low micromolar vs. low nanomolar K_d values). This reduced affinity is probably due to conformational imperfections of the OmpA scaffold, although we cannot exclude that residues not from the loops are additionally involved in binding. This argues for the fact that the exact loop arrangement is of utmost importance, and that already seemingly small deviations from an ideal geometry result in much reduced binding affinities. Therefore, even though OmpA might serve as a convenient platform for displaying the extracellular loops of GPCRs, it may not be possible to modify the system to reproduce *in vivo* binding affinities.

It was previously demonstrated that the N-terminal domain of class A GPCRs are involved in ligand binding, too (Robin-Jagerschmidt et al., 1998; Wieland et al., 1998; Zou et al., 2008). Unfortunately, the topology of OmpA is such that its N-terminus is located on the periplasmic side and hence opposite to the grafted loops. We therefore inserted the sequence of NY1 into the third extracellular loop position of the OmpA scaffold. Because the N-terminus of this receptor domain was still covalently linked to an anchor point, we re-established the free N-terminus of NY1 by proteolytic cleavage with a site-specific protease after refolding/insertion of the chimeric Y1-OmpA protein into the DHPC micelle. Interestingly, in certain detergent micelles the cleaved construct was sufficiently stable even at elevated temperatures (47°C) to allow for extended NMR experiments.

The chemical shift mapping experiments using ^{15}N-NPY with the cleaved Y1L3-NY1 chimeric receptor revealed a different binding mode of both versions of this protein when compared to Y1L3. Again, chemical shift changes were exclusively observed in the C-terminal α-helix of NPY, but appeared clustered on the hydrophobic side of the helix. This indicates that the primary binding region is the same for all constructs, whereas the exact binding mode is changed by the presence of NY1.

Materials and methods

Materials

^{15}N-H_4Cl was from Spectra Stable Isotopes (Andover, MA, USA). DHPC was from Avanti Polar Lipids (Alabaster, AL, USA). All other chemicals were from Sigma-Aldrich (Buchs, Switzerland).

All primers were purchased from Microsynth (Balgach, Switzerland). Primers for deletions were purchased as desalted oligos and used without further purification. Primers for the insertion constructs were self-made by PCR using two short, desalted oligos. PCR products were purified with a Sigma PCR clean-up kit (NA1020-1KT) and used in subsequent QuikChange mutagenesis reactions. The sequences of all constructs were confirmed by dideoxy sequencing (Sanger et al., 1977) by Synergene Biotech GmbH (Zurich, Switzerland).

Cloning and purification of the Blc-derived constructs

The cDNA sequence of the human Y1, Y2 and Y4 receptors as obtained from the Missouri S&T cDNA Resource Center (www.cdna.org) were used as templates for the receptor N-terminal domains without further optimization.

The plasmids coding for the constructs with the NY2 N-terminal domain inserted at positions preceding L11, T14, S20, N32, F34 and L40 were generated from pBlc3 (Schiefner et al., 2010) by an overlapping PCR strategy. The NY2 segment had to be inserted between the OmpA periplasmic signal sequence and the mature Blc sequence. This was achieved by generating via PCR three overlapping constructs comprising (i) the *Xba*I restriction site at the 5′-end of the expression cassette and the OmpA signal sequence (Skerra, 1994); (ii) the Y receptor N-terminal domain; and (iii) the Blc core plus a *Hin*dIII restriction site at the 3′-end of the expression cassette. The fragments were generated by standard PCR procedures using *Vent* DNA polymerase (Fermentas, Thermo Scientific, Wohlen, Switzerland). PCR products were analyzed and purified by 1.5% agarose gel electrophoresis containing ethidium bromide for DNA staining. A QiaGen gel purification kit was used for all PCR purifications. Then, 500 ng of the resulting DNA fragments were digested with *Xba*I (5 U) and *Hin*dIII (10 U) in Tango buffer (Fermentas, Thermo Scientific, Wohlen, Switzerland) at 37°C for 2 h, purified on a 1.5% agarose gel and ligated with the pBlc3 vector backbone, obtained by digestion with *Xba*I and *Hin*dIII. The variants Blc-NY2(T23) and -NY2(P25) were constructed using QuikChange mutagenesis. pBlc3-NY2S20 was used as the starting construct from which three and five residues between the NY2R sequence and the Blc sequence were deleted to generate pBlc3-NY2T23 and pBlc3-NY2P25, respectively. Table S3 in the supplementary material lists all PCR primers that were used.

Calculation of loop mismatch scores between GPCRs and the OmpA scaffold

The overall topology of the loops is defined by 15 unique distances between the anchor points. Likewise, the topology of the 8 anchor points of the 4 extracellular loops of OmpA is defined by 28 unique distances. A total of 24 different modes are possible for arranging 3 foreign loops on the 4 acceptor sites of the scaffold. To rank them according to the similarity with a GPCR structure, a mismatch score was computed based on average distances between the anchor points of the extracellular loops in published GPCR crystal structures (i.e., the C_α atoms of those residues located at the beginning and end of the flanking transmembrane helices) (for a list of the used GPCR coordinates see the supplementary material online).

The C_α atoms of the residues at the beginning and end of the flanking β-strands in the NMR structure of a loop-shortened OmpA variant (2JMM) (Johansson et al., 2007) were considered as the

anchor points of the extracellular loops. Then, the distances between the 6 involved anchor points of the 3 grafted GPCR loops for each of the possible 24 arrangements on the 4 acceptor sites of the OmpA scaffold were calculated and compared to the distances calculated for an average GPCR. Mismatch scores were calculated according to $\sum_{i=1}^{6}\sum_{j=i+1}^{6} d_{i,j}$ with $d_{i,j}$ being the difference in separation distance between the anchor points *i* and *j* corresponding to one loop in an average GPCR and the corresponding distance in OmpA (see also Figure 2).

Synthesis and purification of the neurohormones

The sequences of porcine NPY (pNPY) (Bader et al., 2001) and PYY (pPYY) (Lerch et al., 2004) and of bovine PP (bPP) (Lerch et al., 2002) were used throughout this study.

The synthesis of unlabeled neurohormones was carried out using standard Fmoc-based solid-phase peptide synthesis using an automated system (ABI433A, Applied Biosystems, Carlsbad, CA, USA). ^{15}N-labeled neurohormones were produced as described in detail elsewhere (Bader et al., 2001; Lerch et al., 2002).

All peptide masses were confirmed by ESI-MS.

Biosynthesis and purification of OmpA-based receptor constructs

All genetic deletions/insertions/mutations were performed using the QuikChange mutagenesis method. Table S4 in the supplementary material lists all the primers used. The coding region for the transmembrane domain (TMD) of OmpA from *E. coli* (UniProt entry P0A910 positions 22–346 with a D77E mutation) (Ramakrishnan et al., 2005) served as starting point.

OmpA loop sequences to be replaced with the Y receptor loop sequences were selected based on a previously described loop-shortening study (Koebnik and Kramer, 1995). Residues H19-H31, P62-Y72, K107-G118 and I147-P157 correspond to the extracellular loops 1, 2, 3 and 4, respectively. According to hydrophobicity plots the N-terminal domain and the extracellular loops of the human Y1 receptor (see http://www.gpcr.org/7tm/proteins/npy1r_human) were assumed to comprise the stretches M1-I40, Y100-M112, Q177-S210 and F286-N299. Any cysteines in these sequences were replaced by serines. The cDNA sequences of these loops were optimized by gene synthesis (Microsynth AG, Balgach, Switzerland) to account for optimal *E. coli* codon usage (Kane, 1995; Makrides, 1996). Y receptor N-terminal sequences were as described above.

The chimeric constructs were generated by first deleting all four original OmpA loop sequences, followed by insertion of the foreign Y1 receptor loop sequences via QuikChange mutagenesis. The desired topological arrangement of the Y receptor loops on the OmpA scaffold was achieved in four rounds of mutagenesis, filling three positions with Y1 receptor loops and the fourth one with a minimal turn-inducing sequence (Koebnik, 1999a). The construct carrying the Y1 receptor N-terminus at the position of the third extracellular loop of OmpA (Y1L3-NY1) had the first 40 residues of the human Y1 receptor N-terminally flanked by a $(Gly\text{-}Ser)_3$ spacer as well as the 3C protease (Pallai et al., 1989) cleavage sequence (LEVLFQGP).

OmpA and its derivatives were expressed in *E. coli* BL21(DE3) using the vector pET22b (Novagen, Madison, WI, USA). Unlabeled and ^{15}N-labeled proteins, respectively, were expressed in LB rich medium and M9 minimal medium containing $^{15}NH_4Cl$ as the sole nitrogen source. Cultures were grown at 37°C and induced with 1 mM isopropyl-β-D-thiogalactopyranoside (IPTG) at an OD_{600} of 0.8. Cells were harvested by centrifugation at 4°C and cell pellets were frozen at -20°C until processing.

All chimeric receptor constructs were obtained as inclusion bodies and purified as described previously (Johansson et al., 2007). Inclusion bodies were solubilized in 8 M urea, 10 mM Tris pH 8, 1 mM EDTA to a final protein concentration of 20 mg/ml.

Refolding of chimeric GPCR-OmpA receptors

Buffers for the refolding screens were 10 mM Na-acetate pH 4, 10 mM HEPES/NaOH pH 7, 10 mM Tris/HCl pH 8.8, and 10 mM Na-borate pH 10, always containing 1 mM EDTA. The detergent concentration was chosen to achieve at least a 500-fold excess of detergent over protein or twice the critical micellar concentration (cmc) of the detergent. Protein was added, mixed by vortexing and incubated at 30°C for 5 h. Refolding efficiency was assessed by 'non-denaturing' 18% SDS-PAGE (Schweizer et al., 1978).

The solution was then buffer-exchanged in an Amicon Ultra-4 centrifugal concentrator (10 kDa MWCO; Millipore, Billerica MA, USA; cat. no. UFC801024) to NMR buffer (3% w/v DHPC, 20 mM NaP_i pH 6.5, 100 mM NaCl, 10% v/v D_2O).

3C protease cleavage of Y1L3-NY1

In total, 0.7 mg of 3C protease (for expression and purification of 3C protease see supplementary material online) per mg of Y1L3-NY1 protein was added and the solution was incubated at 4°C for 15 h. 3C protease was removed by incubation with Ni-NTA resin (Sigma, Buchs, Switzerland) at 4°C.

NMR spectroscopy

All spectra were recorded on Bruker AV-600 or AV-700 spectrometers equipped with cryoprobes. Proton chemical shifts were calibrated to the water signal and nitrogen shifts were referenced indirectly to liquid NH_3 (Live et al., 1984).

Proton-nitrogen correlation maps of the receptor constructs were measured as [^{15}N,^{1}H]-TROSY experiments. Raw data were processed using the Bruker Topspin software version 2.0 or 2.1 and transferred to XEASY (Bartels et al., 1995) or CARA (Keller, 2004) for further analysis.

The reported assignments for pNPY (Bader et al., 2001), pPYY (Lerch et al., 2004) and bPP (Lerch et al., 2002) in DPC micelles at pH 4.5 served as the starting points for the assignments of the amide resonances of pNPY, pNPY-R33L and pNPY-R35L, pPYY and bPP in DHPC micelles at pH 6.5 using a strategy reported by our group previously (Bader et al., 2001).

To detect interactions of the hormones with the receptor construct via chemical shift mapping, ^{15}N-labeled neurohormones were dissolved in 0.25 ml NMR buffer and increasing amounts of the refolded receptor constructs (0.5–100 Eq.) were added. In an analogous manner, uniformly ^{15}N-labeled Y1L3 at concentrations between 0.25 and 1 mM was dissolved in NMR buffer and TROSY spectra were recorded at 320 K in the presence of increasing amounts of unlabeled peptide.

On- and off-resonance irradiations in the STD NMR experiment (Mayer and Meyer, 1999, 2001) were applied at -0.5 ppm and 40 ppm, respectively.

Acknowledgments: We thank Simon Jurt for technical assistance during the setup and measurement of NMR experiments, Dr. Geetika Patel for technical assistance with the refolding of the chimeric OmpA receptors and the Forschungskredit of the University of Zurich for funding (grant no. 57132601 to R.W.).

Received June 17, 2012; accepted July 15, 2012

References

Arora, A., Abildgaard, F., Bushweller, J.H., and Tamm, L.K. (2001). Structure of outer membrane protein A transmembrane domain by NMR spectroscopy. Nat. Struct. Biol. *8*, 334–338.

Bader, R. and Zerbe, O. (2005). Are hormones from the neuropeptide Y family recognized by their receptors from the membrane-bound state? ChemBioChem *6*, 1520–1534.

Bader, R., Bettio, A., Beck-Sickinger, A.G., and Zerbe, O. (2001). Structure and dynamics of micelle-bound neuropeptide Y: comparison with unligated NPY and implications for receptor selection. J. Mol. Biol. *305*, 307–392.

Bartels, C., Xia, T.H., Billeter, M., Güntert, P., and Wüthrich, K. (1995). The program XEASY for computer-supported NMR spectral analysis of biological macromolecules. J. Biomol. NMR *5*, 1–10.

Beck-Sickinger, A.G., Wieland, H.A., Wittneben, H., Willim, K.D., Rudolf, K., and Jung, G. (1994). Complete L-alanine scan of neuropeptide Y reveals ligands binding to Y1 and Y2 receptors with distinguished conformations. Eur. J. Biochem. *225*, 947–958.

Bishop, R.E. (2000). The bacterial lipocalins. Biochim. Biophys. Acta *1482*, 73–83.

Bockaert, J. and Pin, J.P. (1999). Molecular tinkering of G protein-coupled receptors: an evolutionary success. EMBO J. *18*, 1723–1729.

Brunet, A.P., Huang, E.S., Huffine, M.E., Loeb, J.E., Weltman, R.J., and Hecht, M.H. (1993). The role of turns in the structure of an α-helical protein. Nature *364*, 355–358.

Campanacci, V., Nurizzo, D., Spinelli, S., Valencia, C., Tegoni, M., and Cambillau, C. (2004). The crystal structure of the *Escherichia coli* lipocalin Blc suggests a possible role in phospholipid binding. FEBS Lett. *562*, 183–188.

Cierpicki, T., Liang, B., Tamm, L.K., and Bushweller, J.H. (2006). Increasing the accuracy of solution NMR structures of membrane proteins by application of residual dipolar couplings. High-resolution structure of outer membrane protein A. J. Am. Chem. Soc. *128*, 6947–6951.

Congreve, M. and Marshall, F. (2010). The impact of GPCR structures on pharmacology and structure-based drug design. Br. J. Pharmacol. *159*, 986–996.

Dennis, M.S. and Lazarus, R.A. (1994). Kunitz domain inhibitors of tissue factor-factor VIIa. I. Potent inhibitors selected from libraries by phage display. J. Biol. Chem. *269*, 22129–22136.

Flower, D.R., North, A.C., and Sansom, C.E. (2000). The lipocalin protein family: structural and sequence overview. Biochim. Biophys. Acta *1482*, 9–24.

Hanson, M.A. and Stevens, R.C. (2009). Discovery of new GPCR biology: one receptor structure at a time. Structure *17*, 8–14.

Houston, M.E.J., Wallace, A., Bianchi, E., Pessi, A., and Hodges, R.S. (1996). Use of a conformationally restricted secondary structural element to display peptide libraries: a two-stranded α-helical coiled-coil stabilized by lactam bridges. J. Mol. Biol. *262*, 270–282.

Hudson, P.J. and Souriau, C. (2003). Engineered antibodies. Nat. Med. *9*, 129–134.

Johansson, M.U., Alioth, S., Hu, K., Walser, R., Koebnik, R., and Pervushin, K. (2007). A minimal transmembrane β-barrel platform protein studied by nuclear magnetic resonance. Biochemistry *46*, 1128–1140.

Kane, J.F. (1995). Effects of rare codon clusters on high-level expression of heterologous proteins in *Escherichia coli*. Curr. Opin. Biotechnol. *6*, 494–500.

Katritch, V., Cherezov, V., and Stevens, R.C. (2012). Diversity and modularity of G protein-coupled receptor structures. Trends Pharmacol. Sci. *33*, 17–27.

Keller, R. (2004). The Computer Aided Resonance Assignment (Goldau, Switzerland: Cantina Verlag).

Kim, H.J., Eichinger, A., and Skerra, A. (2009). High-affinity recognition of lanthanide(III) chelate complexes by a reprogrammed human lipocalin 2. J. Am. Chem. Soc. *131*, 3565–3576.

Kleinschmidt, J.H., Wiener, M.C., and Tamm, L.K. (1999). Outer membrane protein A of *E. coli* folds into detergent micelles, but not in the presence of monomeric detergent. Protein Sci. *8*, 2065–2071.

Kleinschmidt, J.H., Bulieris, P.V., Qu, J., Dogterom, M., and den Blauuwen, T. (2011). Association of neighboring β-strands of outer membrane protein A in lipid bilayers revealed by site directed fluorescence quenching. J. Mol. Biol. *407*, 316–332.

Koebnik, R. (1999a). Membrane assembly of the *Escherichia coli* outer membrane protein OmpA: exploring sequence constraints on transmembrane β-strands. J. Mol. Biol. *285*, 1801–1810.

Koebnik, R. (1999b). Structural and functional roles of the surface-exposed loops of the β-barrel membrane protein OmpA from *Escherichia coli*. J. Bacteriol. *181*, 3688–3694.

Koebnik, R. and Kramer, L. (1995). Membrane assembly of circularly permuted variants of the *E. coli* outer membrane protein OmpA. J. Mol. Biol. *250*, 617–626.

Koshland, D.E. (1958). Application of a theory of enzyme specificity to protein synthesis. Proc. Natl. Acad. Sci. USA *44*, 98–104.

Lagerstrom, M.C. and Schioth, H.B. (2008). Structural diversity of G protein-coupled receptors and significance for drug discovery. Nat. Rev. Drug Discov. *7*, 339–357.

Larhammar, D. (1996a). Evolution of neuropeptide Y, peptide YY and pancreatic polypeptide. Regul. Pept. *62*, 1–11.

Larhammar, D. (1996b). Structural diversity of receptors for neuropeptide Y, peptide YY and pancreatic polypeptide. Regul. Pept. *65*, 165–174.

Larhammar, D. and Salaneck, E. (2004). Molecular evolution of NPY receptor subtypes. Neuropeptides *38*, 141–151.

Lerch, M., Gafner, V., Bader, R., Christen, B., Folkers, G., and Zerbe, O. (2002). Bovine pancreatic polypeptide (bPP) undergoes significant changes in conformation and dynamics upon binding to DPC micelles. J. Mol. Biol. *322*, 1117–1133.

Lerch, M., Mayrhofer, M., and Zerbe, O. (2004). Structural similarities of micelle-bound peptide YY (PYY) and neuropeptide Y (NPY) are related to their affinity profiles at the Y receptors. J. Mol. Biol. *339*, 1153–1168.

Lerch, M., Kamimori, H., Folkers, G., Aguilar, M.-I., Beck-Sickinger, A.G., and Zerbe, O. (2005). Strongly altered receptor binding properties in PP and NPY chimera are accompanied by changes in structure and membrane binding. Biochemistry *44*, 9255–9264.

Live, D.H., Davis, D.G., Agosta, W.C., and Cowburn, D. (1984). Observation of 1000-fold enhancement of ^{15}N NMR via proton-detected multiple-quantum coherences: studies of large peptides. J. Am. Chem. Soc. *106*, 6104–6105.

Makrides, S.C. (1996). Strategies for achieving high-level expression of genes in *Escherichia coli*. Microbiol. Rev. *60*, 512–538.

Mayer, M. and Meyer, B. (1999). Characterization of ligand binding by saturation transfer difference NMR spectrosocpy. Angew. Chem. Int. Ed. *38*, 1784–1788.

Mayer, M. and Meyer, B. (2001). Group epitope mapping by saturation transfer difference NMR to identify segments of a ligand in direct contact with a protein receptor. J. Am. Chem. Soc. *123*, 6108–6117.

Merten, N., Lindner, D., Rabe, N., Rompler, H., Morl, K., Schoneberg, T., and Beck-Sickinger, A.G. (2007). Receptor subtype-specific docking of Asp6.59 with C-terminal arginine residues in Y receptor ligands. J. Biol. Chem. *282*, 7543–7551.

Mierke, D.F., Royo, M., Pellegrini, M., Sun, H.M., and Chorev, M. (1996). Peptide mimetic of the third cytoplasmic loop of the PTH/PTHrP receptor. J. Am. Chem. Soc. *118*, 8998–9004.

Pallai, P.V., Burkhardt, F., Skoog, M., Schreiner, K., Bax, P., Cohen, K.A., Hansen, G., Palladino, D.E., Harris, K.S., Nicklin, M.J., and Wimmer, E. (1989). Cleavage of synthetic peptides by purified poliovirus 3C proteinase. J. Biol. Chem. *264*, 9738–9741.

Pautsch, A. and Schulz, G.E. (1998). Structure of the outer membrane protein A transmembrane domain. Nat. Struct. Biol. *5*, 1013–1017.

Pautsch, A. and Schulz, G.E. (2000). High-resolution structure of the OmpA membrane domain. J. Mol. Biol. *298*, 273–282.

Peeters, M.C., van Westen, G.J., Li, Q., and IJzerman, A.P. (2011). Importance of the extracellular loops in G protein-coupled receptors for ligand recognition and receptor activation. Trends Pharmacol. Sci. *32*, 35–42.

Pham, T.C., Kriwacki, R.W., and Parrill, A.L. (2007). Peptide design and structural characterization of a GPCR loop mimetic. Biopolymers *86*, 298–310.

Ramakrishnan, M., Qu, J., Pocanschi, C.L., Kleinschmidt, J.H., and Marsh, D. (2005). Orientation of β-barrel proteins OmpA and FhuA in lipid membranes. Chain length dependence from infrared dichroism. Biochemistry *44*, 3515–3523.

Reithmeier, R.A. and Bragg, P.D. (1974). Purification and characterization of heat-modifiable protein from the outer membrane of *Escherichia coli*. FEBS Lett. *41*, 195–198.

Ried, G., Koebnik, R., Hindennach, I., Mutschler, B., and Henning, U. (1994). Membrane topology and assembly of the outer membrane protein OmpA of *Escherichia coli* K12. Mol. Gen. Genet. *243*, 127–135.

Robin-Jagerschmidt, C., Sylte, I., Bihoreau, C., Hendricksen, L., Calvet, A., Dahl, S.G., and Benicourt, C. (1998). The ligand binding site of NPY at the rat Y1 receptor investigated by site-directed mutagenesis and molecular modeling. Mol. Cell. Endocrinol. *139*, 187–198.

Sanger, F., Nicklen, S., and Coulson, A.R. (1977). DNA sequencing with chain-terminating inhibitors. Proc. Natl. Acad. Sci. USA *74*, 5463–5467.

Schiefner, A., Chatwell, L., Breustedt, D.A., and Skerra, A. (2010). Structural and biochemical analyses reveal a monomeric solution state of the bacterial lipocalin, Blc. Acta Cryst. Sect. D *66*, 1308–1315.

Schonfeld, D., Matschiner, G., Chatwell, L., Trentmann, S., Gille, H., Hulsmeyer, M., Brown, N., Kaye, P.M., Schlehuber, S., Hohlbaum, A.M., et al. (2009). An engineered lipocalin specific for CTLA-4 reveals a combining site with structural and conformational features similar to antibodies. Proc. Natl. Acad. Sci. USA *106*, 8198–8203.

Schulz, G.E. (2002). The structure of bacterial outer membrane proteins. Biochim. Biophys. Acta *1565*, 308–317.

Schweizer, M., Hindennach, I., Garten, W., and Henning, U. (1978). Major proteins of the *Escherichia coli* outer cell envelope membrane. Interaction of protein II with lipopolysaccharide. Eur. J. Biochem. *82*, 211–217.

Skerra, A. (1994). Use of the tetracycline promoter for the tightly regulated production of a murine antibody fragment in *Escherichia coli*. Gene *151*, 131–135.

Skerra, A. (2000a). Engineered protein scaffolds for molecular recognition. J. Mol. Recogn. *13*, 167–187.

Skerra, A. (2000b). Lipocalins as a scaffold. Biochim. Biophys. Acta *1482*, 337–350.

Smith, G.P., Patel, S.U., Windass, J.D., Thornton, J.M., Winter, G., and Griffiths, A.D. (1998). Small binding proteins selected from a combinatorial repertoire of knottins displayed on phage. J. Mol. Biol. *277*, 317–332.

Surrey, T. and Jähnig, F. (1992). Refolding and oriented insertion of a membrane protein into a lipid bilayer. Proc. Natl. Acad. Sci. USA *89*, 7457–7461.

Tamm, L.K., Abildgaard, F., Arora, A., Blad, H., and Bushweller, J.H. (2003). Structure, dynamics and function of the outer membrane protein A (OmpA) and influenza hemagglutinin fusion domain in detergent micelles by solution NMR. FEBS Lett. *555*, 139–143.

Tyndall, J.D. and Sandilya, R. (2005). GPCR agonists and antagonists in the clinic. Med. Chem. *1*, 405–421.

Walker, P., Munoz, M., Martinez, R., and Peitsch, M.C. (1994). Acidic residues in extracellular loops of the human Y1 neuropeptide Y receptor are essential for ligand binding. J. Biol. Chem. *269*, 2863–2869.

Walser, R., Kleinschmidt, J.H., and Zerbe, O. (2011). A chimeric GPCR model mimicking the ligand binding site of the human Y1 receptor studied by NMR. ChemBioChem *12*, 1690–1693.

Wieland, H.A., Eckard, C.P., Doods, H.N., and Beck-Sickinger, A.G. (1998). Probing of the neuropeptide Y-Y1-receptors interaction with anti-receptor antibodies. Eur. J. Biochem. *255*, 595–603.

Wu, B., Chien, E.Y., Mol, C.D., Fenalti, G., Liu, W., Katritch, V., Abagyan, R., Brooun, A., Wells, P., Bi, F.C., et al. (2010). Structures of the CXCR4 chemokine GPCR with small-molecule and cyclic peptide antagonists. Science *330*, 1066–1071.

Wu, Y., Punta, M., Xiao, R., Acton, T.B., Sathyamoorthy, B., Dey, F., Fischer, M., Skerra, A., Rost, B., Montelione, G.T., et al. (2012). NMR structure of lipoprotein YxeF from *Bacillus subtilis* reveals a calycin fold and distant homology with the lipocalin Blc from *Escherichia coli*. PLoS One *7*, e37404.

Yeagle, P.L., Alderfer, J.L., and Albert, A.D. (1997a). Three-dimensional structure of the cytoplasmic face of the G protein receptor rhodopsin. Biochemistry *36*, 9649–9654.

Yeagle, P.L., Alderfer, J.L., Salloum, A.C., Ali, L., and Albert, A.D. (1997b). The first and second cytoplasmic loops of the G-protein receptor, rhodopsin, independently form β-turns. Biochemistry *36*, 3864–3869.

Zou, C., Kumaran, S., Markovic, S., Walser, R., and Zerbe, O. (2008). Studies of the structure of the N-terminal domain from the Y4 receptor, a G-protein coupled receptor, and its interaction with hormones from the NPY family. ChemBioChem *9*, 2276–2284.

Zou, C., Kumaran, S., Walser, R., and Zerbe, O. (2009). Properties of the N-terminal domains from Y receptors probed by NMR spectroscopy. J. Pept. Sci. *15*, 184–191.